Chaos in a double pendulum

Troy Shinbrot, Celso Grebogi, Jack Wisdom, and James A. Yorke

---

Articles you may be interested in

Quantum chaos in a double barrier heterostructure
J. Appl. Phys. **80**, 247 (1996); 10.1063/1.362811

Ray chaos of underwater sound in longrange propagation
AIP Conf. Proc. **375**, 231 (1996); 10.1063/1.51020

Use of the computer for research on student thinking in physics
Am. J. Phys. **64**, 557 (1996); 10.1119/1.18154

Chaos in a simple impact oscillator: The Bender bouncer
Am. J. Phys. **64**, 397 (1996); 10.1119/1.18254

Nonlinear plasma evolution and sustainment in the reversed field pinch
Phys. Fluids B **4**, 611 (1992); 10.1063/1.860471

Chaos in a double pendulum

Troy Shinbrot

Institute for Physical Science and Technology and Department of Physics, University of Maryland, College Park, Maryland 20742

Celso Grebogi

Laboratory for Plasma Research, University of Maryland and Institute for Physical Science and Technology and Department of Mathematics, University of Maryland, College Park, Maryland 20742

Jack Wisdom

Department of Earth and Atmospheric Sciences, Massachusetts Institute of Technology, Cambridge, Massachusetts 02139

James A. Yorke

Institute for Physical Science and Technology and Department of Mathematics, University of Maryland, College Park, Maryland 20742

A novel demonstration of chaos in the double pendulum is discussed. Experiments to evaluate the sensitive dependence on initial conditions of the motion of the double pendulum are described. For typical initial conditions, the proposed experiment exhibits a growth of uncertainties which is exponential with exponent $\lambda = 7.5 \pm 1.5$ s^{-1}. Numerical simulations performed on an idealized model give good agreement, with the value $\lambda = 7.9 \pm 0.4$ s^{-1}. The exponents are positive, as expected for a chaotic system.

I. INTRODUCTION

Sensitive dependence on initial conditions is the hallmark of chaos.[1] This means that tiny separations, $\Delta x(t_0)$, between nearby initial conditions are amplified exponentially in time t:

$$\Delta x(t) \sim \Delta x(t_0) e^{\lambda t}, \tag{1}$$

where $\Delta x(t)$ is the separation[2] between nearby trajectories and λ is some positive constant. The double pendulum provides a simple yet dramatic demonstration of this growth. A double pendulum[3] is made from two pendula attached end to end as shown in Fig. 1. Despite its simplicity, it exhibits extremely wild and unpredictable[4] behavior. In this study we demonstrate that the underlying cause of this behavior, namely the exponential growth given in Eq. (1), can be experimentally and numerically evaluated for the double pendulum.

We begin in Sec. II by describing a simple and direct qualitative demonstration of chaos in the double pendulum. Then, in Sec. III, we discuss the root cause of the observed behavior. In the following section we describe a quantitative experiment which can be used to evaluate the rate of exponential growth, and in Sec. V we discuss results obtained from the experiment. Finally, we draw conclusions.

II. THE TANDEM DOUBLE PENDULUM

A dramatic demonstration of the growth of separations in initial conditions intrinsic to chaotic motion can be produced by putting two identical[5] double pendula in tandem, as sketched in Fig. 2.

If the pendula are released from the same small initial angle, they will oscillate in phase for long periods of time. In Fig. 3, we show actual photographs of our pendula just before release and 30 s after release. The pendula trajectories have stayed together for this entire time. The motion of the pendula is predictable and periodic.

If the pendula are released from a larger initial angle, however, the trajectories quickly diverge from one another. This is demonstrated in Fig. 4, where we show photographs of the pendula just before release from a large initial angle and 2 s after release. Clearly, the pendula trajectories have moved far apart. The motion here is unpredictable and chaotic.

We stress that these results are intrinsic to the chaotic nature of the double pendulum and are not due to imperfections[6] in the double pendula or to particulars of the mechanisms of releasing the pendula. Even if the pendula were exactly identical, we could not release the pendula with the infinite precision necessary to disregard Eq. (1). *Any* difference in initial conditions, however tiny, is sufficient to give rise to the growth in separations shown in Fig. 4.

We also remark that sturdy construction of the tandem pendula base effectively isolates the double pendula from one another.[7] The behavior observed can be fully discussed
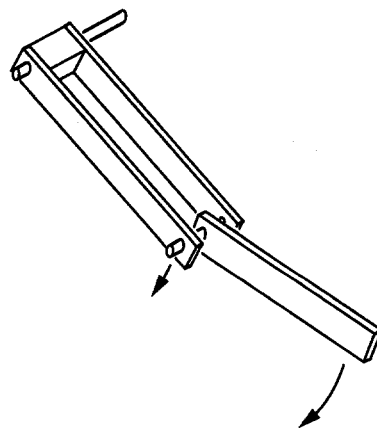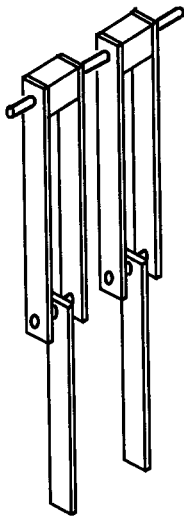

Fig. 1. A double pendulum.

Fig. 2. Tandem double pendula.

(a)

(b)

Fig. 3. Small angle motion: (a) release from small initial angle; (b) positions 30-s later.

assuming that no coupling exists between the two double pendula.

III. CAUSE OF EXPONENTIAL GROWTH

The growth in separations just described can occur in many extremely simple systems. For example, consider the well-known case of the logistic equation. Imagine that we want to study the ecology of a population of lions and gazelles living on a particular prairie. Let L_n be the fraction of lions in the nth generation. Thus if there were 10 lions and 9990 gazelles in the first generation, L_1 would be 1/1000. Now if L_n is small, the lions will have plenty of gazelles to feast upon, and their population will grow. We can therefore write that

$$L_{n+1} = \widehat{G}L_n, \tag{2}$$

where $\widehat{G}$ is some constant which defines the growth rate; say $\widehat{G} = 4$. Thus the number of lions will quadruple every generation in the presence of a plentiful food supply. Once L_n becomes large, however, the number of gazelles becomes limited, and the lion population can no longer grow at its prior rate. We can easily include this in our model by making the growth rate G decrease as the lion population grows. The simplest such model would be to write $G = G(1 - L_n)$, where G is some new constant; again say $G = 4$. Thus our final model is

$$L_{n+1} = G(1 - L_n)L_n. \tag{3}$$

This is known as the logistic equation. Although quite simple, it exhibits features of a chaotic system. If we take our prior starting point, $L_1 = 1/1000$, and look at populations after successive generations, we obtain the pattern shown in Fig. 5. While L_n remains small, the population nearly quadruples every generation, but once L_n becomes substantial, the behavior becomes extremely erratic and unpredictable. This is because in the logistic model, like the double pendulum, small separations grow exponentially in time.

To observe this growth, let us suppose that the initial gazelle population were 9991 instead of 9990. This tiny, 0.01%, discrepancy in L_1 would grow with every generation as shown in Fig. 6, until about ten generations, when
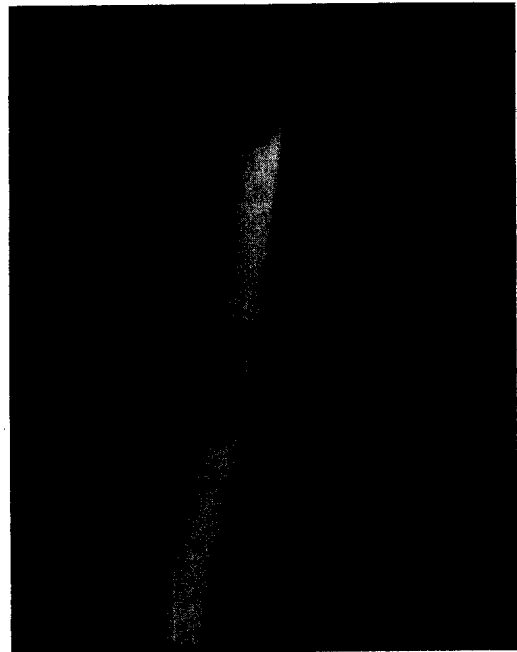
the discrepancy would become 100%. That is, if we are certain of our initial conditions to within 0.01%, we can predict the outcome for only ten generations. After that point, the system will be completely unpredictable. Notice that Fig. 6 is plotted on a semilog scale. Since the plot is roughly linear on this scale, we know that growth must be roughly exponential in time on average, i.e.,

$$\Delta L_n = \Delta L_1 e^{\lambda n}, \tag{4}$$

where $\lambda \cong 1.35$ for Fig. 6. This means that if we wanted to double the time for which our system remains predictable, we would have to square the initial accuracy. Since our initial accuracy in L_1 was 1 part in 10,000, to maintain
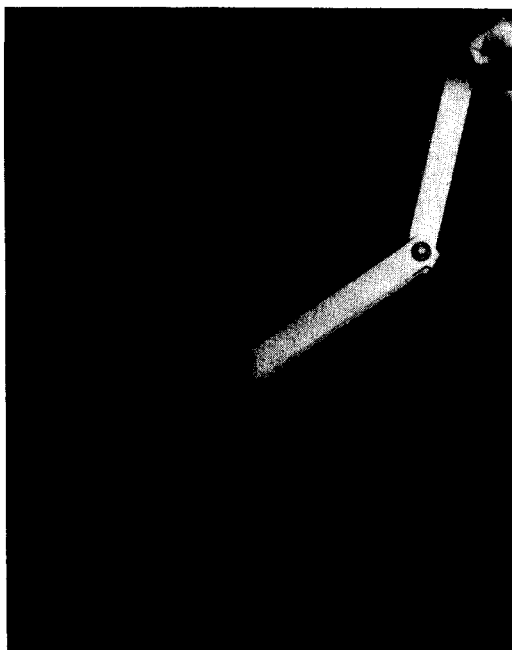
(a)
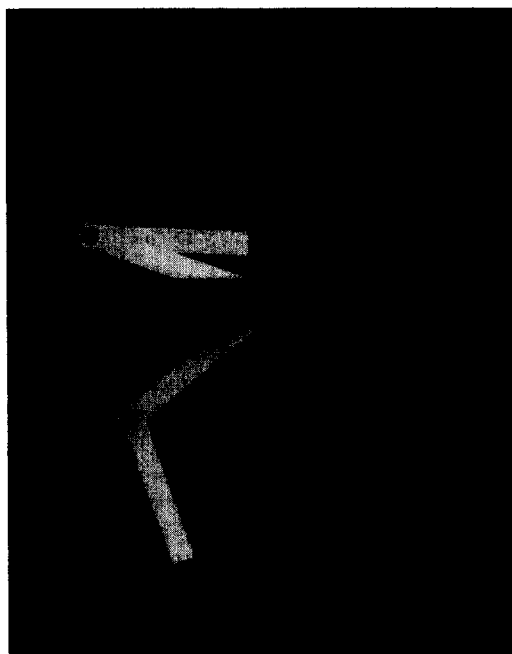
(b)

Fig. 4. Large angle motion: (a) release from large initial angle; (b) positions 2-s later.
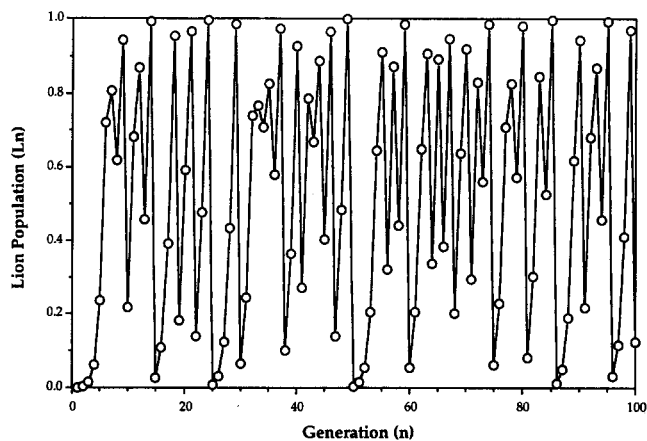

Fig. 5. Number of lions predicted in successive generations.

the state of another double pendulum—or the same pendulum during another trial—be X_2. We can expand the equations of motion in powers of $\Delta X = X_1 - X_2$ to give

$$\Delta \overset{\circ}{X} = A_1 \Delta X + O(|\Delta X|^2) \tag{5}$$

where A_1 is some matrix. If we start the two double pendula off at very close to the same initial condition, then $|\Delta X|$ will be small, and we can neglect higher-order terms, leaving

$$\Delta \overset{\circ}{X} = A_1 \Delta X. \tag{6}$$

The eigenvectors a_i of Eq. (6) adhere to

$$a_i(t) = a_i(t_0)e^{\lambda_i t}, \tag{7}$$

where $i = 1$ to 4.

If the largest λ_i, denoted λ, is positive, we say that the motion is unstable, since fluctuations grow rapidly with time and move the two pendula away from one another. On the other hand if λ is negative, fluctuations will rapidly vanish, and we say that the motion is stable, and the two pendula will stay nearly in synch. Stable motion is insensitive to fluctuations and tends to be predictable; conversely unstable motion tends to be unpredictable.

A good working definition of a chaos is the following. A system is said to be chaotic if the eigenvalue λ—called the Lyapunov exponent—is positive for typical initial conditions. Such a system exhibits exponential growth of distur-

predictability for 20 generations, we would require 1 part in 100,000,000 accuracy, for 40 generations we would require 1 part in 10,000,000,000,000,000 accuracy, and so forth. It is evident that no amount of initial accuracy will be sufficient to predict the outcome for long times. This is the reason that exponential growth leads to unpredictable behavior.

The origin of this exponential growth in separation between trajectories in continuous systems, like the double pendulum, can be understood in the following way. Suppose that the state of one double pendulum at time t_0 is defined by the vector X_1, which would contain four components: two angles and two angular speeds. Likewise, let
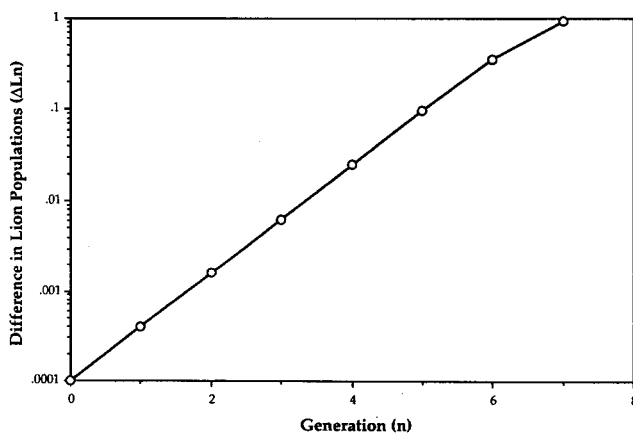

Fig. 6. Exponential growth in separations in predicted number of lions.

bances. It should be remarked that a displacement ΔX typically has components in the directions of all of the $\mathbf{a}_i$, yet as time passes, the growth in the direction with the largest positive exponent will quickly swamp the growth in other directions. This largest exponent thus dominates the exponential rate of growth, so we include only this exponent in Eq. (1). Local variations[9] in the Lyapunov exponent are to be anticipated, but we expect to see (1) govern the long time behavior of the system.

Here it is important to stress that the Lyapunov exponent can be expected to depend on the state of the system— i.e., the positions and speeds of the two pendula.[10] Thus the exponent can locally be either negative or positive. In a chaotic system, disturbances will continually grow despite local variations. In nonchaotic systems, by contrast, disturbances can locally grow, but on average they will remain fixed. This distinction is well illustrated by considering a single, ordinary pendulum. It is easily proved[11] that a single pendulum cannot be chaotic. Yet if the pendulum is released from two nearby initial conditions, both nearly vertical, the trajectories will at first quickly separate. A short time later, however, they will converge, completely compensating for the earlier separation. It is a straightforward and worthwhile exercise for the student to verify by numerical experiment[12] that the time averaged exponential rate of separation for a single pendulum is zero, while for a double pendulum (released from a large initial angle), it is positive.

For small initial angles of the double pendulum, on the other hand, approximations can be made which make the equations of motion nearly linear.[13] In that case, the motion becomes (nearly) predictable. The physical reason for this is that for small angles, the pendula oscillate about the rest position. This oscillation is stable and consequently predictable.

IV. MEASUREMENT OF EXPONENT

A. Physical experiment

To analyze chaos quantitatively, just one double pendulum is needed. In this case, we release the double pendulum from, as nearly as possible, the same initial condition several times. We then measure, by a simple technique that we will describe shortly, the separation between these several
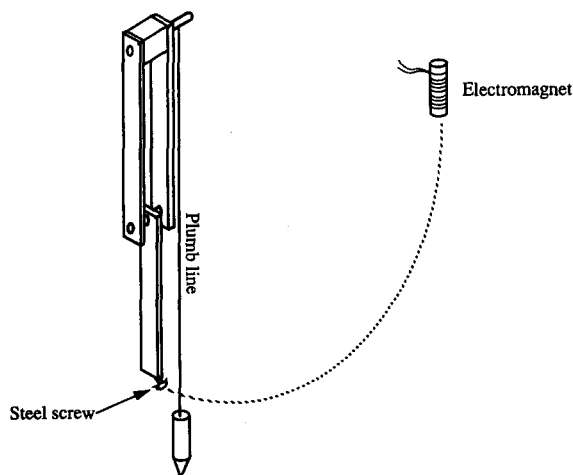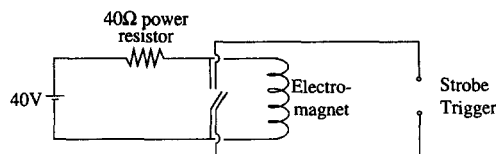

Fig. 7. Apparatus.

Fig. 8. Electrical schematic.

trajectories as time elapses. By plotting these separations as a function of time, we derive the exponent defined in Eq. (1).

A double pendulum[14] was constructed as shown in Fig. 7 and clamped to a solid bench to ensure isolation from unwanted influences. The room was then darkened and illumination was provided with an externally triggered strobe light set to flash 25 times per second. The background behind the scene and the pendulum were painted flat black and 2 mm wide[15] white stripes were taped along the exposed pendula sides to provide visibility. A Polaroid® camera was used to photograph the stroboscopic trajectory of the double pendulum. Small parallax errors were minimized by centering the camera on the scene.

A white plumb line was suspended from the upper axle of the pendulum. The plumb line gives a reference angle needed to accurately measure the angles of each pendulum. The pendulum was held in its initial position by an electromagnet which attracted the steel screw shown in the figure. The electromagnet was clamped to a laboratory stand, fixing its position in space. By means of a double throw switch, the electromagnet released the pendulum at the same time that the strobe was triggered. An electrical schematic is shown in Fig. 8.

The completed photographs were mounted on a drafting table and the angles of each pendulum were measured, aligning the plumb line to be exactly vertical. A drafting machine[16] accurate to within 0.2° was used to measure each successive angular position. Taking the grain of the photograph into account, an estimated final accuracy of 1° was obtained.

B. Numerical experiment

In addition to the physical experiment, a numerical simulation was performed in which the equations of motion[17] were integrated by the fourth order Runge–Kutta–Nystrom method.[18] To ensure correspondence between physical and numerical experiments, the moments of inertia of the numerical double pendulum were set equal to those of the physical double pendulum. The latter were calculated after measuring the appropriate masses and lengths. Noise and dissipation[19] were neglected in the numerical experiment.

V. RESULTS

Typical results[20] of several experimental trials, each consisting of releasing the double pendulum as nearly as possible from the same initial position, are shown in Fig. 9. The initial position was chosen to have large pendula angles and so to exhibit chaotic motion. In the figure we plot the Euclidean distance in $(\vartheta_1, \vartheta_2, \dot{\vartheta}_1, \dot{\vartheta}_2)$ space[21] between successive points taken at the same time after release from the different trials. Also shown, as a bold line, is the result of comparing separations produced in numerical simulations[22] of a double pendulum programmed to have parameters identical with the physical pendulum.
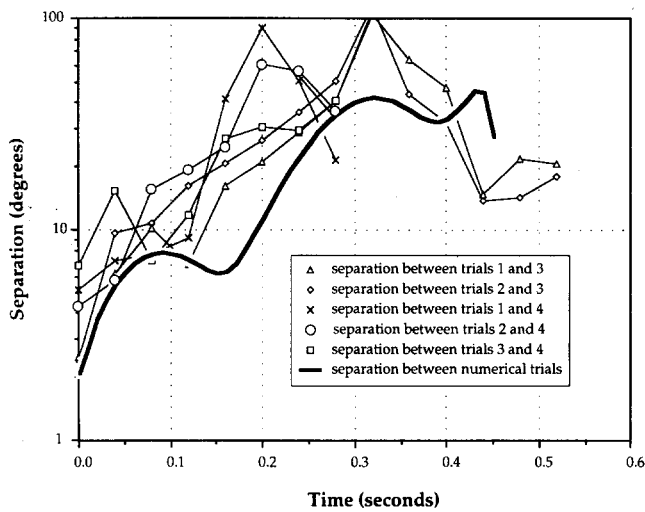
Fig. 9. Experimental results from typical initial condition; bold curve is numerical result.

In addition to the clear upward trend seen in the curves shown in Fig. 9, it is notable that a substantial undulation is present in both the physical and the numerical experiments. Earlier, we mentioned that local variations in λ may be anticipated; here we see an illuminating example of the source of these variations. By examining the pendula trajectories, shown in Fig. 10, we see that just after being released, the outer pendulum *oscillates* about its vertical position. Ordinarily, this would be an *unstable* position, however the influence of the inner pendulum pulling the outer pendulum down is such that this position becomes *stable*. The sign of the Lyapunov exponents dictates stability, thus apparently during this period of time at least one of the exponents has changed from positive to negative. The occurrence of this particular change is due to the accidental choice of initial state; nevertheless it illuminates the richness of the dynamics of the double pendulum.

Further analysis was performed to compare the physical and numerical experiments. Since Fig. 9 contains large undulations, the slope of any of the curves in the figure must depend on the range of points used. Therefore it was considered prudent to create an objective criterion for the choice of points. From the definition of the Lyapunov ex-

ponent [Eqs. (1) and (5)], the magnitude of separations between different trajectories should be as small as possible. Thus we must not discard any points near $t = 0$, where the separation is smallest. To decide when to stop taking points, we adopt the following procedure.[23] We examine successive numbers of points, perform a least-squares fit of the points to our expected exponential form, and calculate the reduced chi-squared for the fit. We then select the largest possible number of points which gives a minimum value of chi-squared. By this technique, we arrive at the results shown[24] in Table I.

We can then calculate an average of the Lyapunov exponent, weighted in accordance to the displayed uncertainties, which gives[25] $\lambda = 7.5 \pm 1.5$ s^{-1}. We can similarly compute the exponent which minimizes χ_r^2 for the numerical simulation, resulting in the value $\lambda = 7.9 \pm 0.4$ s^{-1}. It is worth remarking that for chaotic systems, each realization of the Lyapunov exponent is intrinsically nonreproducible, thus some uncertainty in the final estimate is unavoidable. Moreover, we must reiterate that in any real experiment, the exponential rate of separation can only be averaged over a finite time,[26] while to prove that a system is chaotic, one must technically average over an infinite time span. Consequently, no experiment can definitively prove that a given system is chaotic. Nevertheless, it is fair to say that our experimental results are fully consistent with the observed chaotic behavior of the the double pendulum.

VI. CONCLUSION

Using the double pendulum, we have successfully measured the exponential rate of separation of nearby trajectories which is characteristic of chaotic systems. The results obtained show good agreement between experiment and numerical simulation and give estimates of the Lyapunov exponent with respectable uncertainties. Most important, the Lyapunov exponent obtained by either method is unequivocally positive, as expected for a chaotic system.

The level of these experiments seems appropriate for graduate or upper level undergraduate Physics students. For more advanced students, the experiments can be extended by varying the initial energy of the pendula in a search for a transition region between nearly linear and chaotic motion.[27]
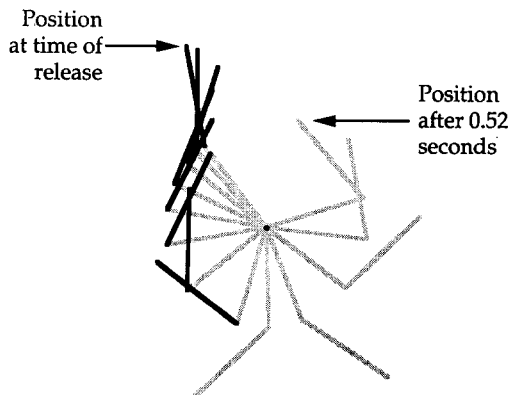
ACKNOWLEDGMENTS

Fig. 10. Reproduction of actual stroboscopic positions of pendula (from data, first initial condition, Trial 1). Notice solid lines oscillate about vertical.
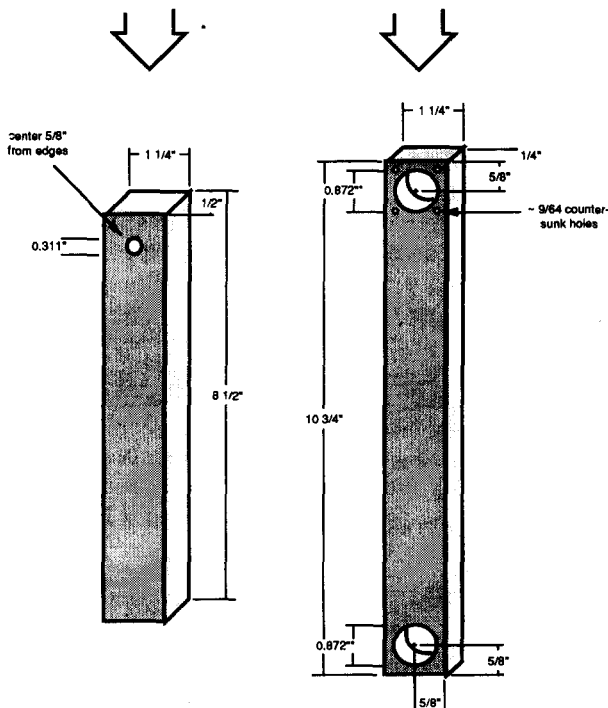
APPENDIX A: PLANS FOR DOUBLE PENDULUM

Parts list for one pendulum

Quantity	Item (all units are inches)
2	$\frac{1}{4} \times 1\frac{1}{2} \times 11$ aluminum bar stock
1	$\frac{1}{2} \times 1\frac{1}{2} \times 8\frac{1}{2}$ aluminum bar stock
1	$1 \times 1\frac{1}{4} \times 1\frac{1}{4}$ aluminum bar stock
1	$\frac{5}{16}$ o.d. $\times 1\frac{7}{8}$ CRS or stainless rod stock
1	$\frac{5}{16}$ o.d. $\times 3\frac{1}{2}$ CRS or stainless rod stock
2	$\frac{1}{4}$ i.d. E-rings
1	$1 \times 2 \times 2$ CRS bar stock
4	High precision bearings (e.g., roller skate bearings)
1	$\frac{3}{8}$ i.d. $\times \sim 3$ fiberglass or similar for sleeves (excess length allowed to fit in lathe chuck)
8	$\frac{1}{2} \times 8 - 32$ flat head machine screws

Assembly:
(sleeves, E-rings, screws not shown)
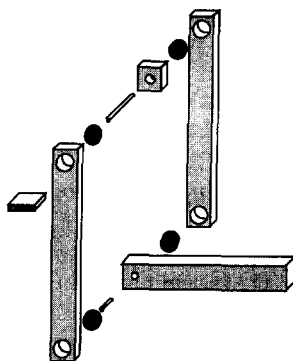
Material: Aluminum bar stock

Quantity: 1   Quantity: 2

Material: Cold Rolled Steel   **Material: Cold Rolled Steel**
Quantity: 1   Quantity: 1
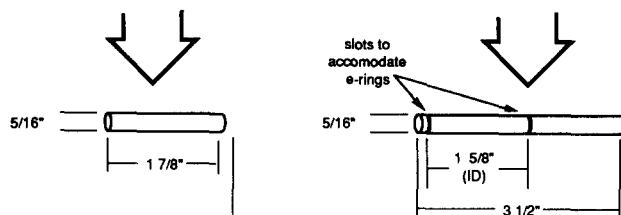
Material: Aluminum   **Material: Fiberglass or similar**
Quantity: 1   Quantity: 2
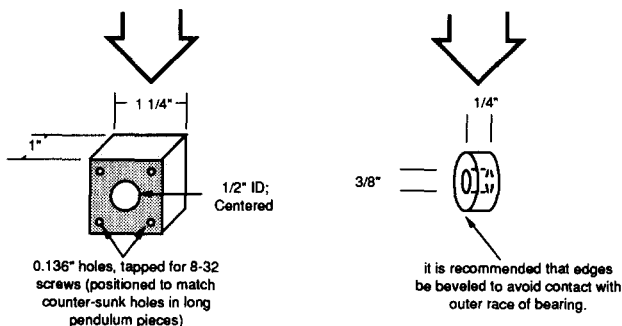
Material: Cold Rolled Steel
Quantity: 1
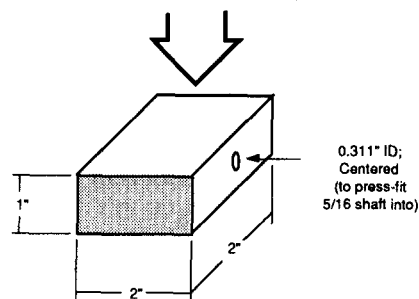
APPENDIX B: EQUATIONS OF MOTION FOR DOUBLE PENDULUM

In this appendix we derive the equations of motion for the double pendulum. We consider pendula with masses m_1 and m_2 and lengths l_1 and l_2 as shown in Fig. B1. We let ϑ_1 and ϑ_2 denote the angles displaced from equilibrium.

The potential energy is easily verified to be

Fig. B1. Definitions.

$$V = l_1(1 - \cos\vartheta_1)m_1 g + [l_1(1 - \cos\vartheta_1)$$
$$+ l_2(1 - \cos\vartheta_2)]m_2 g, \qquad (B1)$$

while the kinetic energy is

$$T = \tfrac{1}{2}(m_1 + m_2)l_1^2\dot\vartheta_1^2 + \tfrac{1}{2}m_2 l_2^2\dot\vartheta_2^2$$
$$+ m_2 l_1 l_2 \dot\vartheta_1 \dot\vartheta_2 \cos(\vartheta_1 - \vartheta_2). \qquad (B2)$$

The Euler–Lagrange equations of motion then give

$$\cos(\Delta\vartheta)\ddot\vartheta_1 + (l_2/l_1)\ddot\vartheta_2 = \dot\vartheta_1^2 \sin(\Delta\vartheta) - (g/l_1)\sin\vartheta_2, \qquad (B3)$$

$$\cos(\Delta\vartheta)\ddot\vartheta_2 + (\mu l_1/l_2)\ddot\vartheta_1$$
$$= -\dot\vartheta_2^2 \sin(\Delta\vartheta) - (g\mu/l_2)\sin\vartheta_1, \qquad (B4)$$

where $\Delta\vartheta \equiv \vartheta_1 - \vartheta_2$ and $\mu \equiv 1 + (m_1/m_2)$. These equations can be separated to produce

$$\ddot\vartheta_1 = \frac{g(\sin\vartheta_2 \cos(\Delta\vartheta) - \mu\sin\vartheta_1) - (l_2\dot\vartheta_2^2 + l_1\dot\vartheta_1^2 \cos(\Delta\vartheta))\sin(\Delta\vartheta)}{l_1(\mu - \cos^2(\Delta\vartheta))}, \qquad (B5)$$
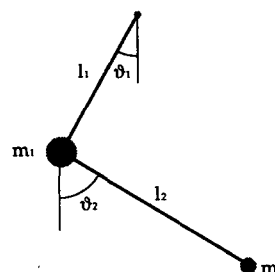
$$\ddot\vartheta_2 = \frac{g\mu(\sin\vartheta_1 \cos(\Delta\vartheta) - \sin\vartheta_2) + (\mu l_1\dot\vartheta_1^2 + l_2\dot\vartheta_2^2 \cos(\Delta\vartheta))\sin(\Delta\vartheta)}{l_2(\mu - \cos^2(\Delta\vartheta))}. \qquad (B6)$$

Equations (B5) and (B6) are highly nonlinear and can only be integrated numerically, yielding a time series, or trajectory, of values for ϑ_1, ϑ_2, $\dot\vartheta_1$, and $\dot\vartheta_2$.

For small oscillations, the dynamics of the double pendulum change. In this case, we use small angle approximations for the trigonometric functions, yielding

$$\ddot\vartheta_1 \cong g(\vartheta_2 - \mu\vartheta_1)/l_1(\mu - 1), \qquad (B7)$$

$$\ddot\vartheta_2 \cong g\mu(\vartheta_1 - \vartheta_2)/l_2(\mu - 1). \qquad (B8)$$

These are coupled linear oscillator equations discussed in any standard classical dynamics text. The equations are linear and will therefore produce regular motion. Thus we expect that the exponential rate of growth of fluctuations should become vanishingly small as the initial displacements of the pendula are reduced.[28]

APPENDIX C: DATA

Trials following beginning from (as nearly as possible) the same initial condition. Fewer points taken from trials 4 and 5 because the first three trials revealed that minimum χ_r^2 slope requires < 15 points.

Time×25 (s)	ϑ_1 (deg)	ϑ_2 (deg)
	Trial 1	
1	141.7	169.8
2	136.9	179.6
3	127.8	197.5
4	114.8	202.2
5	98.7	205.9
6	78.9	205.0
7	50.6	180.5
8	15.7	127.1
9	− 2.3	47.2
10	− 2.3	− 57.2
11	− 22.0	− 135.1
12	− 52.8	− 189.8
13	− 83.1	− 220.0
14	− 106.6	− 231.2
15	− 121.0	− 233.0

	Trial 2	
1	141.1	169.3
2	137.0	179.1
3	129.4	182.6
4	117.4	190.3
5	100.8	204.0
6	97.5	205.6
7	55.1	186.3
8	22.7	140.2
9	− 1.8	66.2
10	− 1.8	− 38.0
11	− 18.0	− 120.8
12	− 48.1	− 182.0
13	− 78.7	− 216.1
14	− 103.3	− 233.2
15	− 120.0	− 235.4

	Trial 3	
1	142.6	170.3
2	140.0	179.5
3	131.7	192.1
4	120.9	204.0
5	106.2	209.9
6	91.6	196.1
7	63.0	157.2
8	30.0	90.9
9	− 1.0	7.9
10	− 4.2	0.0
11	− 10.0	− 102.3
12	− 38.5	− 189.1
13	− 71.7	− 216.6
14	− 99.9	− 245.5
15	− 119.1	− 260.2

	Trial 4	
1	141.2	168.8
2	137.1	171.7
3	128.6	197.3
4	115.4	206.4
5	98.7	202.3
6	103.0	204.9
7	50.5	179.3
8	17.1	128.5
9	− 3.8	50.2
10	− 22.3	− 56.0

	Trial 5	
1	141.1	169.1
2	139.8	175.2
3	132.0	197.7
4	120.5	208.6
5	105.9	209.6
6	123.6	192.7
7	22.2	146.3
8	6.8	108.0
9	− 7.5	31.0

$(\vartheta_1,\vartheta_2,\mathring{\vartheta}_1,\mathring{\vartheta}_2)$—space separations between trials (deg)

Time× 25 (s)	Trials 1 and 2	Trials 2 and 3	Trials 1 and 3	Trials 1 and 4	Trials 2 and 4	Trials 3 and 4	Trials 1 and 5	Trials 2 and 5	Trials 3 and 5	Trials 4 and 5
1	1.0	2.4	2.5	7.0	6.9	6.8	5.2	4.3	3.9	4.3
2	14.5	9.6	6.2	11.0	23.3	15.4	7.1	5.8	10.8	5.4
3	15.3	10.7	10.1	4.5	14.8	7.1	7.6	15.5	5.7	4.2
4	15.8	16.3	6.9	8.9	24.1	11.8	9.1	19.4	6.7	7.8
5	16.9	20.7	16.3	24.6	8.1	27.2	41.6	24.8	32.5	25.8
6	23.9	26.5	21.2	34.2	13.1	30.9	89.3	60.6	79.9	58.3
7	10.7	36.3	29.4	3.2	9.7	29.8	50.8	56.2	53.6	48.7
8	17.3	51.1	41.2	3.9	14.1	41.3	21.6	36.5	33.8	23.9
9	19.0	112.6	104.3	18.9	24.6	108.1				
10	20.1	44.0	63.7							
11	16.2	32.6	47.5							
12	9.9	13.9	14.9							
13	8.4	14.2	21.8							
14	4.5	18.0	20.9							

[1] For a nice introduction to this subject, the reader is referred to D. Ruelle, "Strange attractors," Math. Intelligencer 2, 126–137 (1980).

[2] Technically, this separation is measured in phase space.

[3] Plans for a double pendulum appear in Appendix A.

[4] P. H. Richter and H. J. Scholz, "The planar double pendulum," Film C1574 (Naturwiss. Ser. 9, No. 7/C1574) Publ. Wiss. Film, Sekt. Techn. Wiss., Göttingen, 1986, and related models in P. H. Richter, "Die Theorie des Kreisels in Bildern," Report 226, Inst. Dyn. Syst., Univ. Bremen, 1990.

[5] The double pendula we used were made as nearly identical as possible by keeping all pairs of components clamped together during machining.

[6] The pendula are manifestly nearly identical, for trajectories did *not* separate when the pendula were released from small angles. Even modest differences would prevent the pendula from oscillating in phase for 30 or more seconds.

[7] This can be verified by releasing only one of the pendula from a moderate angle. Coupling would cause sympathetic oscillations—which were not observed in our apparatus—in the second, stationary, pendulum.

[8] Technically, the term Lyapunov exponent applies in the limit as $|\Delta X| \to 0$ and $t \to \infty$. Since these limits are not realized in practical experiments, we will not make this distinction.

[9] These variations are ubiquitous; notice that Fig. 6 shows variations from linearity even for the simple logistic model.

[10] We will discuss a particular instance of this phenomenon shortly.

[11] A good discussion appears in G. L. Baker and J. P. Gollub, *Chaotic Dynamics, An Introduction* (Cambridge U.P., New York, 1990), pp. 7–9.

[12] The student should be cautioned to choose initial conditions with the same energy. Failing to do this will result in a secular growth in separations which will unnecessarily complicate the problem.

[13] See Appendix B.

[14] Plans in Appendix A.

[15] The stripes were chosen to be the minimum thickness that would produce clear images when photographed. The strobe flash rate was determined so as to maximize the number of exposures captured for later analysis. A faster rate would produce overlap between the thin white stripes in successive exposures.

[16] Photographs were also digitized and angles evaluated by computer, however, the drafting machine was found to be faster and equally accurate.

[17] See Appendix B.

[18] Numerical integration for the double pendulum problem is discussed in D. R. Stump, "Solving classical mechanics problems by numerical integration of Hamilton's equations," Am. J. Phys. 54, 1096–1100 (1986).

[19] This is justifiable in that dissipation could have little effect in the first $\frac{1}{2}$ s that we had to work with in the physical experiment.

[20] Typical results shown to reduce clutter in figure. Data from all trials appear in Appendix C.

[21] In our programs, conjugate momenta were computed automatically, so actual phase space distances could be calculated as well. However, the expressions for the momenta required many cumbersome calculations which necessarily reduced accuracy. For this study we chose to opt for simplicity over rigor in distance calculations.

[22] Several different variations from the nominal initial condition were ex-

amined. Lyapunov exponents were virtually identical, hence only one simulation curve is shown. The separations shown differ initially by 1% in both ϑ_1 and ϑ_2.

[23] In less advanced classroom or laboratory settings, less rigorous techniques can of course be used. For example, all points $<\frac{1}{4}$ s from release can be examined. Some accuracy will be lost, but the goal of the experiment—measurement of a positive exponent—would still be achievable.

[24] The uncertainties shown are statistical uncertainties from least-squares fits and do not account for variations between trials.

[25] Uncertainty shown is standard error of weighted average.

[26] This is known in the literature as the problem of finite time estimation; see P. Grassberger, R. Badii, and A. Politi, "Scaling laws for invariant measures on hyperbolic and non-hyperbolic attractors," J. Stat. Phys. 51, 135–178 (1988) or E. Ott, C. Grebogi, and J. A. Yorke, "Theory of first order phase transitions for chaotic attractors of non-linear dynamical systems," Phys. Lett. A 135, 343–348 (1989).

[27] This has been done in our laboratory, confirming that small initial angles give approximately periodic motion with $\lambda \cong 0$, while initial angles larger than about 30° give chaotic motion with $\lambda > 0$.

[28] For a good discussion of the limitations of neglecting nonlinear terms in two oscillator systems, the reader is referred to G. H. Walker and J. Ford, "Amplitude instability and ergodic behavior for conservative nonlinear oscillator systems," Phys. Rev. 188, 416–432 (1969).

Quantum mechanical tunneling in an ohmic contact

J. Crofton, P. A. Barnes, and M. J. Bozack
Solid State Sciences Laboratory, Department of Physics, Auburn University, Auburn, Alabama 36849

The tunneling probability for majority carriers in an ohmic contact to n-type GaAs has been calculated by directly solving the Schrödinger equation for the wave functions in the semiconductor depletion region. The direct solution is straightforward and relies on fewer assumptions than previous calculations based on the WKB approximation. It also provides a useful application of undergraduate quantum mechanics to an important area of VLSI semiconductor technology. The direct solution can be performed on an 80286 machine in less than a minute and yields tunneling probabilities roughly twice as large as the WKB approximation at most electron energies. The tunneling probability is then used to calculate the contact resistance as a function of doping for the contact. The contact resistances are approximately one-half the resistances calculated using the WKB method.

I. INTRODUCTION

When a metal is deposited upon a semiconductor surface, either an ohmic or a rectifying contact is formed, depending on the shape of the current–voltage (I–V) behavior of the contact. This paper focuses on ohmic contacts, defined as contacts which have a linear and symmetrical I–V characteristic. Ohmic contacts are used in applications requiring interconnects which do not distort the shape of a signal, and in cases where precise measurement of semiconductor device parameters is important. In such cases, the voltage drop across the ohmic contact must be negligible compared to the voltage drop across a device connected to the contact.

Ohmic contacts can be made by depositing a metal with a work function less than the work function of an n-type semiconductor or greater than the work function of a p-type semiconductor.[1] Very few metal-semiconductor combinations exist which satisfy this requirement. The vast majority of ohmic contacts involve a thin layer of very heavily doped semiconductor material immediately adjacent to the metal to make the depletion layer sufficiently thin that carriers can readily tunnel through it. A common example of an ohmic contact is Al on p-type or heavily doped n-type Si. The doping level required for good ohmic contact is usually in excess of 10^{19} atoms/cm^3.

Theoretical modeling of ohmic contacts depends upon calculations of the quantum mechanical tunneling probability of majority carriers through the energy barrier in the semiconductor depletion layer at the metal–semiconductor junction. Since tunneling is the predominant mechanism which leads to low resistance ohmic contacts to semiconductors, accurate calculation of the tunneling probability is helpful for understanding experimentally measured current densities and contact resistances in real contacts. We present here a straightforward determination of the tunneling probability through a parabolic barrier characteristic of the metal–semiconductor junction in an ohmic contact. The calculation can be performed at the level of undergraduate quantum mechanics and demonstrates how to predict the tunneling probability and ultimately the contact resistance of an ohmic contact.

II. THE WKB SOLUTION TO THE TUNNELING PROBABILITY

The WKB approximation[2,3] can be used to provide an approximate solution to the Schrödinger equation provided the potential energy $U(x)$ changes slowly over a de-Broglie wavelength. For a particle of mass m and energy E moving with a potential energy $U(x)$, the Schrödinger equation for the stationary states has the usual form

$$-(\hbar^2/2m)\nabla^2\psi(x) + U(x)\psi(x) = E\psi(x). \qquad (1)$$

The WKB solution to this equation can be written in the